2018-03-01

In Vitro Label Free Screening of Chemotherapeutic Drugs Using Raman Micro-Spectroscopy: Towards a New Paradigm of Spectralomics.

Zeineb Farhane
Technological University Dublin

Haq Nawaz
Technological University Dublin

Franck Bonnier
Université Francois-Rabelais de Tours

See next page for additional authors

Recommended Citation

Farhane, Z. et al. (2018). In Vitro Label Free Screening of Chemotherapeutic Drugs Using Raman Micro-Spectroscopy: Towards a New Paradigm of Spectralomics.*Journal of Biophotonics*, vol. 11, no. 3, e201700258. DOI: 10.1002/jbio.201700258

Funder: SFI

In vitro label free screening of chemotherapeutic drugs using Raman micro-spectroscopy: towards a new paradigm of spectralomics.

Z. Farhane[1,2*], H. Nawaz[3], F. Bonnier[4], H.J. Byrne[1]

[1]FOCAS Research Institute, Dublin Institute of Technology, Kevin Street, Dublin 8, Ireland.

[2]School of Physics, Dublin Institute of Technology, Kevin Street, Dublin 8, Ireland.

[3]Department of Chemistry, University of Agriculture, Main Rd. Faisalabad, Pakistan.

[4]Université François-Rabelais de Tours, Faculty of Pharmacy, EA 6295 Nanomédicaments et Nanosondes, 31 avenue Monge, 37200 Tours, France.

*Corresponding author: zeineb.farhane@mydit.ie

Abstract:

This overview groups some of the recent studies highlighting the potential application of Raman micro-spectroscopy as an analytical technique in preclinical development to predict drug mechanism of action and in clinical application as a companion diagnostic and in personalised therapy due to its capacity to predict cellular resistance and therefore to optimise chemotherapeutic treatment efficacy.

Notably, the anthracyclines, Doxorubicin and Actinomycin D, elicit similar spectroscopic signatures of subcellular interaction characteristic of the mode of action of intercalation. Although Cisplatin and Vincristine show markedly different signatures, at low exposure doses, their signatures at higher doses show marked similarities to those elicited by the intercalating anthracyclines, confirming that anticancer agents can have different modes of action with different spectroscopic signatures, depending on the dose.

The study demonstrates that Raman micro-spectroscopy can elucidate subcellular transport and accumulation pathways of chemotherapeutic agents, characterise and fingerprint their mode of action, and potentially identify cell resistant strains. The consistency of the spectroscopic signatures for drugs of similar modes of action, in different cell lines, suggests that this fingerprint can be considered a "spectralome" of the drug-cell interaction suggesting a new paradigm of representing spectroscopic responses.

Keywords: Raman micro-spectroscopy, cancer cells, chemotherapeutic drugs, mechanism of action, cellular resistance, spectralomics

1. Introduction:

Vibrational spectroscopy can perform cellular imaging in a (benchtop) microscopic geometry, and can provide non invasive label free screening of, for example, nanoparticle or drug uptake, trafficking and interaction mechanisms, as well as cellular responses and toxicity [1-5], eliminating the need for multiple assays in toxicological screening and drug discovery and preclinical screening stages, by elaborate robotic High Content Analysis systems. Vibrational spectroscopy has also been demonstrated for diagnostics applications, *in vivo* and *ex vivo*, in tissue [6, 7], cells [8, 9] and body fluids [10, 11]. A further potential application which is currently attracting increasing attention is in understanding and screening cellular resistance to therapeutic treatments to guide strategies for personalised therapies [12, 13].

Both Infrared absorption (IR) and Raman spectroscopy can be performed on live cells [14, 15], although the significantly lower contribution of water in the latter favour it for live cell analysis [10]. Raman micro-spectroscopy also provides superior spatial resolution to IR spectroscopy, being an optically based microscopy technique, commonly employed in a confocal mode, enabling subcellular analysis of biological processes at an organelle level [15]. Raman spectral maps of whole live cells can be performed over minutes to hours, but in cases where spectral quality is favoured over speed, for detailed analysis, measurement protocols often entail fixing the cells at fixed time points after exposure to exogenous agents, for example radiation or toxicants, having optimised protocols for cell fixation [16]. Both IR and Raman spectroscopy have been used to assess the effects of drugs on cells, demonstrating their potential to measure changes in a high throughput manner and therefore can be used in drug screening [17-19]. Many studies have reported the use of vibrational spectroscopy to monitor the effects of anticancer agents, including polyphenols [20] cardiotonic steroids [21], and platinum compounds [22], on cancer cells, and Hughes *et al*. [17], Mignolet *et al.* [23] and Jamieson and Byrne [24] have recently reviewed the potential for vibrational micro-spectroscopy as a label free *in vitro* platform for screening the mechanisms of action and efficacies of candidate drugs at the discovery and pre-clinical screening stages. The development of such *in vitro* screening techniques is particularly pertinent at present, given the increasing legislative pressure to develop *in vitro* alternatives to animal models for scientific research and product development as prioritised by the EU Directive-2010/63/EU on the replacement, reduction and refinement of animal experimentation.

Using Fourier Transform IR (FTIR) microscopy, Derenne *et al.* demonstrated that drugs of similar mode of action have similar spectroscopic signatures [19], indicating potential

applications in pre-clinical screening of the mode of action of new candidate drugs. Analysis of spectral variations in prostate cell lines, induced by drug exposure, clustered drugs classified as anti-microtubules (methotrexate, mercaptopurine), anti-topoisomerases (vincristine, vinblastine, paclitaxel) and anti-metabolites (doxorubicin, daunorubicin) separately. Derenne *et al.* further demonstrated that the spectral changes were not cell line specific, but were consistent over seven different cell lines [25]. Mignolet *et al.* [23] reviewed the body of work exploring IR signatures of anti-cancer drugs inside cancer cells and changes induced after drug exposure, including the effects of cell cycle and cell culture model, arguing that FTIR can be employed for screening of new drug candidate molecules for known or unknown modes of action.

Using Raman spectroscopy, subcellular resolution can be achieved due to the high spatial resolution achievable with optical microscopy, allowing intracellular organelles to be resolved. Raman spectra are also typically recorded at higher spectral resolution than IR spectra, and therefore more detailed biochemical information can be gained [26], with more potential for elucidating 'modes of action' by analysis of the detailed spectral changes. El-Mashtoly *et al*. [27] demonstrated the capability of Raman spectroscopy for monitoring the distribution of the distinct structure of erlotinib, containing a carbon-carbon triple bond, and its metabolic products in colorectal adenocarcinoma SW480 cells. Le Roux *et al*. [28] explored cell death routes after exposure to gold based metallodrugs. Salehi *et al.* [29, 30] and Feofanov *et al.* [31] probed the resonance Raman response to detect and study cellular responses after exposure to paclitaxel, and the nonfluorescent transition-metal complex, Theraphtal, respectivelly. Draux *et al.* [32] investigated the effect of Gemcitabine on cell biomolecules in the lung cancer cell line Calu-1, after 48hrs exposure. Moritz *et al.* [33] used laser tweezers Raman spectroscopy to study the effects of doxorubicin on leukaemia cells and demonstrated that drug exposed cells exhibited an increase in DNA features after prolonged exposure time. Schie *et al.* [34] also investigated the effect of doxorubicin on malignant lymphocytes at late stages, from 24 to 96 hrs, while G*uo et al.* [35] explored the effects of doxorubicin on malignant hepatocytes after 12 hrs exposure, showing a decrease in DNA features and an increase in proteins and lipids features. Hartmann *et al.* [36] studied the effect of Docetaxel on human breast adenocarcinoma cell line MCF-7 comparing the treated cells with the untreated ones and investigating the cellular morphological changes induced by the chemotherapeutic drug. Lin *et al.* [37] used Raman spectroscopy to assess the cytotoxicity of Paclitaxel in CA46, human Burkitt's lymphoma cells. Zoladek *et al.* [38] showed the potential of Raman micro-spectroscopy for

label free time course imaging (at 2 hrs intervals over 6 hrs) of live human breast cancer cell (MDA-MB-231) undergoing apoptosis after exposure to etoposide.

In monitoring the response to exogenous agents *in vitro*, it has also been demonstrated that both FTIR and Raman spectroscopy can potentially be employed to understand cellular resistance pathways in different cell lines. Cellular resistance pathways were specifically targeted by Yosef *et al.* [39] who used Raman spectral imaging to investigate the oncogenic mutation resistance to epidermal growth factor receptor targeting therapy and colon cancer cells with and without oncogenic mutations such as KRAS and BRAF mutations were treated with erlotinib , an inhibitor of epidermal growth factor receptor, in order to detect the impact of these mutations on Raman spectra of the cells as markers of cell resistance. Rutter *et al.* [40] utilised a cell cloning technique to specifically isolate sensitive and resistant cells from a mixed cell population, and investigated the difference in response of gemcitabine-sensitive and gemcitabine-resistant Calu-1 epidermoid lung cancer cells to the commercial drug, using IR spectroscopy. Furthermore, Siddique *et al.* [41] showed that it was also possible to identify differences of nilotinib-sensitive and nilotinib-resistant K562 (a chronic myelogenous leukaemia cell line) cloned cells, using both FTIR and Raman microspectroscopies. The ability of vibrational spectroscopy to characterise and differentiate responses of resistant and sensitive cell types to drugs opens up potential clinical applications as a Companion Diagnostics (CD) tool, and ultimately personalised medicine approaches [42, 43]

Although the potential of *in vitro* spectroscopic screening of cellular processes has been well demonstrated, research has been somewhat fragmented, lacking in coherence and standardisation of measurement protocols. Critically, the analysis and interpretation of the spectral responses remains a challenge, even in the hands of "specialists". At the recent Faraday Discussions [44], the question as to what extent individual spectral features can be assigned to specific molecular responses, given the complex nature of the samples under investigation, featured highly. By their very nature, label free techniques register all species within the sampling area, and identification of specific responses requires more sophisticated techniques to data-mine the differential responses due to cell injury or change. Regression and correlation approaches can be employed to extract the specific spectroscopic signatures of cellular changes which are correlated with external stimuli, and, for example independently elucidate the spectroscopic signatures of the direct chemical effects of the stimulus from the subsequent cellular metabolic responses. In the case of chemotherapeutic agents, the uptake, distribution and accumulation, chemical interactions and subsequent cellular metabolic responses can be

monitored [17, 18]. Nevertheless, these differential spectral responses remain multivariate in nature, and contain contributions of the multitude of biochemical constituents involved. The conditioned thinking, based on a labelled approach, is to search for specific "Biomarkers". However, it is becoming increasingly apparent that the spectral response can have (additive) contributions of increased or decreased concentrations of constituent biomolecules, but also more complex contributions due to conformational, environmental (pH etc.) changes, and that identification of the (differential) spectroscopic signature, rather than specific bands associated with specific biomolecules, may be more appropriate. For realistic applications potential, however, it is important that these combinatorial signatures are characteristic of the cellular interaction and/or response pathway, and are translatable across cell lines and ultimately patient samples. Although Derenne *et al.* demonstrated that drugs of similar mode of action have similar spectroscopic signatures using FTIR microscopy [19], there have been few other studies which have attempted to demonstrate consistency between spectroscopic signatures of drug interactions and cellular responses [3, 24]. The identification of specific spectral signatures which are common for drug mechanisms of action and cellular responses opens the perspective to a new "spectralomics" paradigm, in label-free fingerprinting and monitoring of biological processes in cells *in vitro* using Raman spectroscopy, with potential applications in fundamental cytological research, pre-clinical pharmacological development, and ultimately improved individualised clinical therapeutics

Herein, the results of a number of independent studies of the action of chemotherapeutic agents *in vitro* are gathered and reviewed, with a view towards assessment of the consistencies of spectroscopic signatures of the subcellular interactions of the drugs, and the subsequent cellular responses. Specifically, Raman micro-spectroscopic studies of the subcellular interactions of Doxorubicin (DOX), Actinomycin D (ACT), Cisplatin (Cisp) and Vincristine (Vinc) in human lung cancer cell lines, and their subsequent responses, are considered. The dose response profiles are examined in the context of classical cytotoxicological screening assays.

2. Cytotoxicity assays and their limits

A range of cytotoxicological assays are commonly employed to measure the *in vitro* responses of cell populations, including cell proliferation, viability and toxicity, after exposure to external agents such drugs, nanoparticles or radiation. Amongst these are the tetrazolium bromide

(MTT), Alamar Blue (AB) and Neutral Red (NR) assays, each of which targets different aspects of the response pathway.

NR is a fluorometric dye, which measures the lysosomal activity using 3-Trimethyl-2,8-phenazinediamine, monohydrochloride, which binds to the lysosomes of viable cells after penetration by passive diffusion due to its cationic charge. This uptake depends on the ability of the cell to maintain a pH gradient by production of ATP. Therefore, the dye cannot penetrate inside dead cells and the amount of retained dye is proportional to the number of viable cells. [45, 46] The MTT test is a colorimetric assay that measures the reduction of yellow 3-(4, 5-dimethythiazol-2-yl)-2, 5-diphenyl tetrazolium bromide (MTT) by mitochondrial succinate dehydrogenase into purple formazan crystals, insoluble in aqueous solution [47, 48]. Succinate dehydrogenase or succinate-coenzyme Q reductase (SQR) or respiratory Complex II is an enzyme complex, bound to the inner mitochondrial membrane of mammalian mitochondria and many bacterial cells. It is the only enzyme that participates in both the citric acid cycle and the electron transport chain, so the MTT assay is the reflection of mitochondrial activity.

Alamar blue (AB), on the other hand, is a water-soluble dye and one of the most highly used cytotoxicity assays for *in vitro* quantification of the cell viability[49].When added to cell cultures, the active dye, resazurin or 7-hydroxy-10-oxidophenoxazin-10-ium-3-one, diffuses into the cytosol and acts as an intermediate electron acceptor allowing the oxidised blue non-fluorescent form to be reduced by both mitochondrial and cytosolic enzyme activity to the fluorescent pink form which is easily measured by its absorption or fluorescence. [47-49]

Both AB and NR are considered an expression of general cellular metabolism and, while reduced conversion compared to controls is used as a measure of reduced cellular viability for both AB and MTT assays, the MTT response is more specifically sensitive to mitochondrial enzymes while AB is related to both mitochondrial and cytosolic activities.

Quantitatively, the cytotoxic response is commonly quoted in terms of the effective concentration with elicits 50% of the maximum response of the cell population to the exogenous agent (IC_{50}), determined through dose-response curves. However, toxicity studies are commonly conducted at different time points, using different cell lines, leading to a lack of consistency in toxicological data for chemotherapeutic agents. Figure 1 shows, for example the accumulated cytotoxicity data as measured using the MTT assay, for Cisp [18] and Vinc [50] in A549, human lung adenocarcinoma cells, and DOX [51] and ACT [52] in both A549 and Calu 1, a human lung epidermoid carcinoma cell line, at differing time points. The inverse IC_{50}, as a comparative measure of the toxicity [53], is plotted against the exposure time. For the case of DOX, the toxicity increases monotonically as a function of exposure time. The two cell lines

show comparable results, although that of A549 seems to saturate at prolonged exposures. In the case of ACT, although negligible response was observed at 24hrs (IC_{50}>50μM), the toxicity at 48 hrs and 72 hrs far exceeds that of DOX, in both cell lines [52]. Cisp also requires a more prolonged exposure time to elicit appreciable responses in A549 [50], while, for the same exposure time, Vinc requires substantially lower concentration to elicit the same toxic response [50].

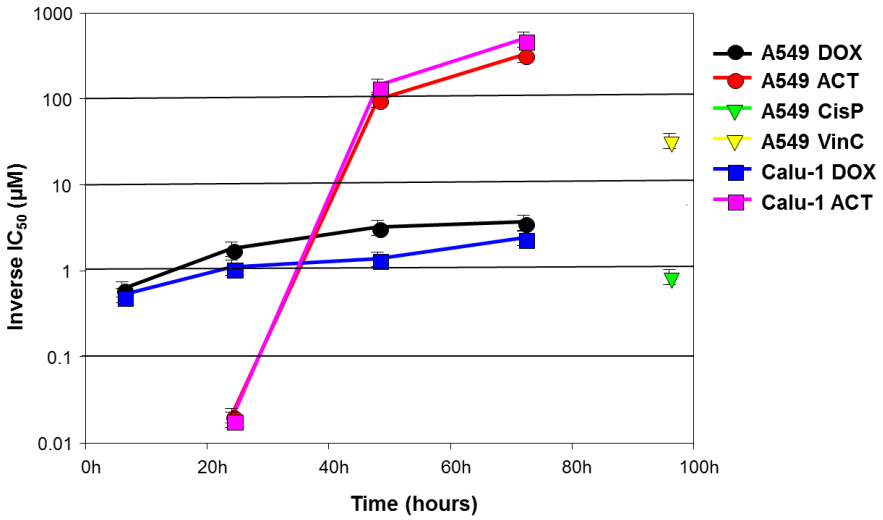

Figure 1: Plot of the inverse IC_{50} against exposure time for DOX and ACT exposure to A549 and Calu-1 cell lines and Vinc and Cisp to the A549 cell line.

Maher *et al.* [45] developed a numerical model to simulate nanoparticle uptake, cytotoxicity and subsequent cellular response and highlighted the fact that differences in the quantitative responses of cytotoxicity assays can arise due to the fact that each assay measures different underlying cellular responses which can occur at different rates. An assessment of the action and efficacy of, for example a chemotherapeutic agent, according to a single endpoint is therefore extremely limited. Computational Modelling approaches to predictive toxicity, such as that of Adverse outcome pathways [54], have sought to deconvolute the action of exogenous agents, in terms of the molecular initiating event (MIE) and the subsequent cascade of key events (KE) that reflect the causal progression from the initial perturbation of the system towards the adverse outcome. In the context of the action of chemotherapeutic drugs *in vitro*, the MIE can be considered the chemical interaction of the drug, for example in the cell nucleus, while the subsequent cascade of events can determine the efficacy of a drug action. Understanding of the chemistry of the MIE can be key to establishing quantitative structure

activity relationships to guide synthetic strategies, while understanding the subsequent pathways may be key to understanding mechanisms of drug resistance and sensitivity in different cell lines and ultimately patients.

Therefore, to have a global idea of the effects of external agents such as drugs or nanoparticles on cells and identify any subsequent cellular responses, there is a need for a more developed label free method which gives a holistic picture of the cascade of events which occurs after cell exposure.

3. Data processing: pre and post processing

To consider vibrational spectroscopy and specifically Raman micro-spectroscopy as an analytical tool for clinical applications, it should be able to address the many challenges related to the complexity of biological samples and their chemical and physical heterogeneity. In this context, data pre and post processing play an important role in dealing with variations in instrumental responses, between different biological samples and improving spectral quality.

Byrne *et al.* [55] summarised the pre-processing steps routinely used to improve recorded spectra quality, and the commonly used post-processing techniques for the classification, discrimination and analysis of data set from biological samples. In fact, many factors, including background coming from sample scattering and/or fluorescence, substrate contributions, specifically when analysing thin samples, and instrumental enhanced scattering contributions, can influence spectra quality and therefore need to be subtracted. In some cases, those factors can be minimised experimentally, for example analysing samples in immersion to reduce laser scattering [6] or use of substrates with negligible Raman scattering [56]. In others cases, there is a need for pre-processing algorithms for background subtraction prior to analysis, using for example a NCLS (non-negatively constrained least squares) [57] or EMSC (extended multiplicative signal correction) algorithm [58]. Spectra are also commonly smoothed to reduce noise using the Savitsky-Golay algorithm or singular value decomposition (SVD) [59], baseline corrected (fifth order polynomial) and vector or area normalised.

After pre-processing, data post-processing or data mining is necessary to detect and analyse changes in spectral profiles associated, for example, with biological process, drug, nanoparticle, radiation exposure etc., mostly in a large and complex data set. The most common method in terms of multivariate spectral data analysis is Principal Components Analysis (PCA), a powerful unsupervised approach for the analysis of large multidimensional data sets, which allows the reduction of the number of variables, although retaining most of the variation within

the dataset. It represents the spectra in data groupings of similar variability, allowing the identification and differentiation of different spectral subgroups. The loadings of the PCs represent the variance for each variable (wavenumber) for a given PC, the order of the PCs denoting their importance to the dataset. PC1 describes the highest amount of variation, and analysis of the loadings can give information about the source of the variability inside a dataset, derived from variations in the molecular components contributing to the spectra.

It has been demonstrated that the PC loadings can be most simply understood when analysis of data subgroups is undertaken in a pairwise fashion [60, 61], whereby the loading of the PC can be interpreted as differences of the biochemical content of the two differentiated datasets [60], highlighting its ability to provide molecular information and biochemical differences of analysed samples. Notably, PCA does not cluster the data, per se, in the same manner as for example Hierarchical or K-Means Cluster Analysis, whereby differential distribution of the data according to negative or positive loadings associates specific spectral features with that dataset.

As an extension to PCA, independent components analysis (ICA) can also be employed as an unsupervised statistical technique to identify latent variables, called independent components, in each data set separately. In the case of Raman micro-spectroscopy, ICA can be used to identify spectral contributions such as those from substrate, which can then be removed or plotted and studied in their own [61, 62].

More sophisticated spectral analysis is required to extract specific information related to an external variable such as exogenous exposure dose or time, requiring supervised methods such Partial Least Squared Regression (PLSR). PLSR is a statistical regression technique which reduces the dimensionality of the data and correlates information, here represented by the spectra data set, to, for example, time evolution or drug concentrations or to a gold standard assay, to track the dependent evolution of the spectral signatures in, for example, subcellular regions. The regression coefficients obtained by PLSR can be analysed and provide information about the contribution of spectral variations. As a function of frequency, the coefficients illustrate the spectral features which are influenced by the external factor selected [63].

4. Raman micro-spectroscopy for chemotherapeutic pre-clinical screening

Raman spectroscopic analysis of drug-cell interactions has focused both on changes in the cellular Raman spectra upon drug application, and also during intracellular tracking of the drug and its metabolites. [1, 27, 51, 52, 64]

Farhane *et al*.[1, 51, 61, 63] used Raman spectroscopy to determine not only the subcellular location of the drug DOX in A549 and Calu- 1 human lung adenocarcinoma cells, but also the differing pharmacodynamics of the drug uptake and subcellular localization, as well as the subsequent cellular responses, over a period 0-72hrs. In fact, using Raman micro-spectroscopy, DOX could be clearly detected in both the nucleolus and surrounding nucleus, while Confocal Laser Scanning Microscopy (CLSM) images show that only the nucleus appears red (compared to the corresponding controls, in which no fluorescence is detected), due to the characteristic DOX fluorescence (Figure 2), the clearly visible dark spots of the nucleoli suggesting that DOX does not accumulate in the nucleoli. However, Raman micro-spectroscopy clearly demonstrates that DOX does accumulate in the nucleoli, indicating that the dark spots are a result of fluorescence quenching in the environment. The study also indicated that DOX selectively targets the RNA in the nucleolus, before the nuclear and cytoplasmic regions.

A.

1. **2.** **3.** **4.** **5.** **6.**

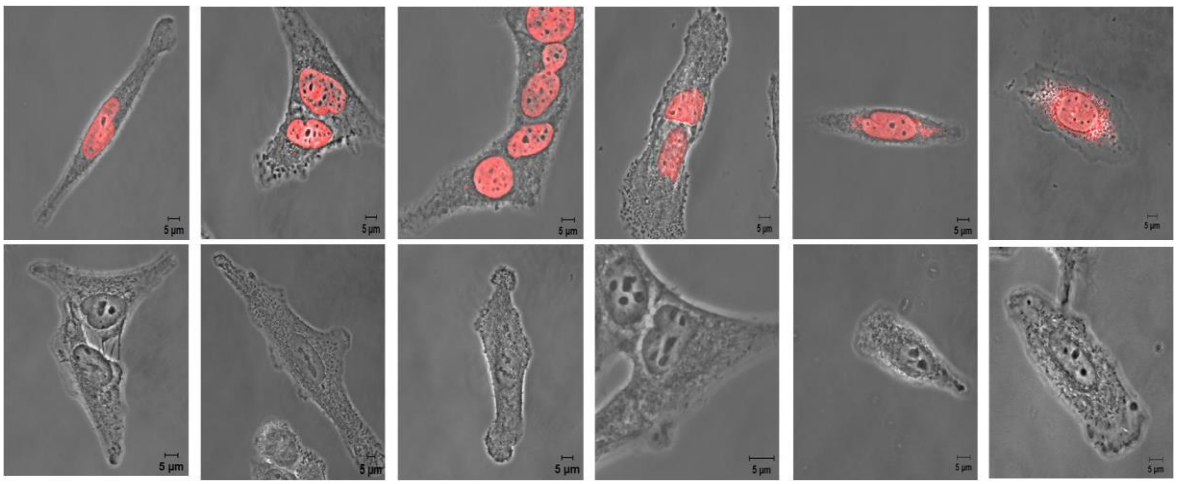

B.

1. **2.** **3.** **4.** **5.** **6.**

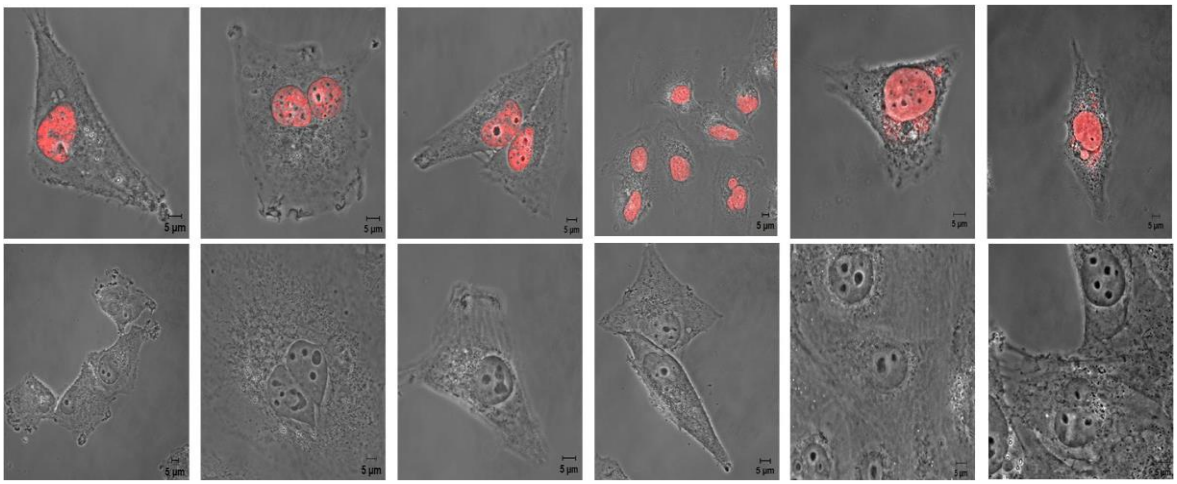

Figure 2: Confocal Laser Scanning Fluorescence images of **A.** A549 cells and **B.** Calu-1 cells after DOX exposure and corresponding controls: **1.**2hrs DOX exposure, **2.**6hrs DOX exposure, **3.**12hrs DOX exposure, **4.**24hrs DOX exposure, **5.**48hrs DOX exposure and **6.**72hrs DOX exposure [63]

Using multivariate data analysis, consisting of PCA, ICA and PLSR, Raman micro-spectroscopy was shown to be capable of tracking the kinetics of the uptake and accumulation of DOX at a subcellular level *in vitro* [51, 63]. Results show that the chemotherapeutic drug accumulates first in, and saturates, the nucleolus, then the nucleus and is only detectable in the cytoplasm at later stages, after nuclear disruption (Figure 3A). Raman micro-spectroscopy can differentiate the biochemical responses associated with the subcellular regions of nucleolus, nucleus and cytoplasm, both in terms of the mechanisms of action (DNA intercalation in nulear area and ROS production in cytoplasmic region), and the subsequent cellular metabolic responses for the same cell lines and between different cell lines (Figure 3B), the faster uptake in Calu-1 cells (Figure 3A) highlighting different cellular kinetics, effects and resistance related to expression of anti-apoptotic proteins and tolerance to DNA damage and implication of DNA repair mechanisms manifest as an increase in DNA signatures at late stages (Figure 3B).

A.

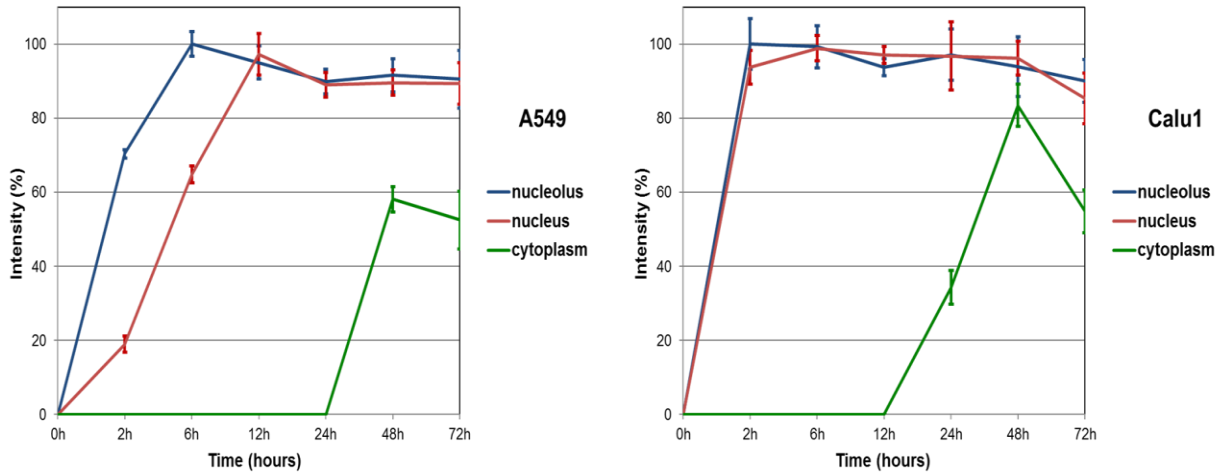

B.

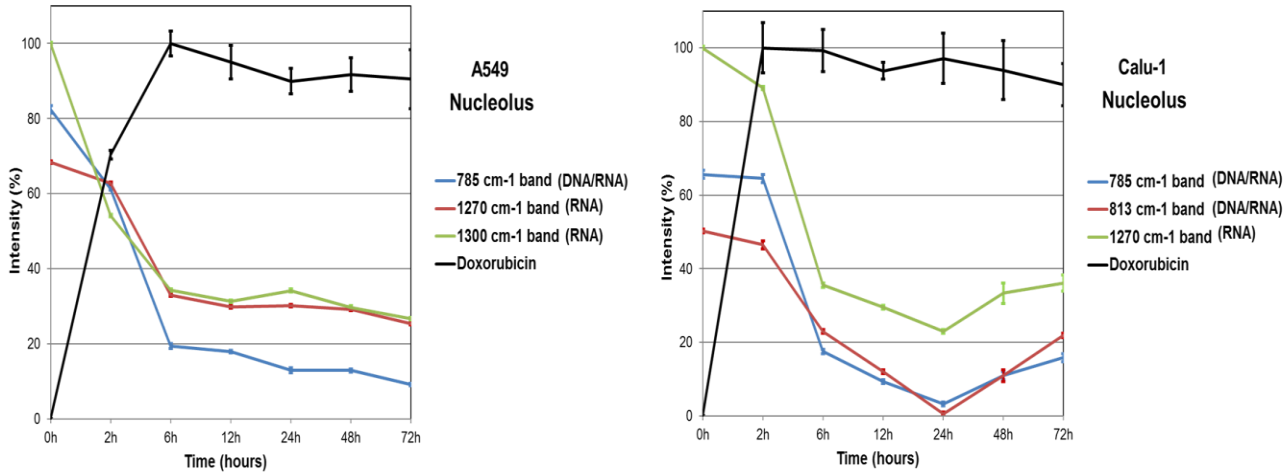

Figure 3: A. Evolution of DOX, represented by the Raman band at 465 cm^{-1}, as a function of time for the A549 and Calu-1 cell line for each cellular compartment, nucleolus, nucleus and cytoplasm. **B.** Evolution of selected DNA and RNA features as function of time.
Intensities are expressed as percentage according to the maximum value over the three cellular compartments for each cell line and standard deviation corresponds to the spectral variations of the Raman band over the 30 measurements per location. [51, 63]

A similar response profile was observed for Actinomycin D (ACT) in the same cell lines, both in terms of time evolution and spectroscopic signatures [52]. In fact, a similar chemical binding signature, related to RNA/DNA interaction, resulting in a decrease of both bands at 785 cm^{-1} (DNA backbone O–P–O) and 813 cm^{-1} (RNA O–P–O phosphodiester band stretching) was observed after DOX and ACT exposure (Figure 4). The substantially slower uptake rate for ACT (48-72hrs) compared to DOX (6-12hrs) may be due to different side chain composition.

Nevertheless, both exploit similar cellular pathways, accumulating first in the nucleolus and then the nucleus, which suggests that the anthracycline chemotherapeutic group targets the nucleolus first, binding with RNA, and nucleus second, binding with DNA, before accumulating in the cytoplasm. This is not the accepted view of the mode of action of anthracycline drugs, which considers only the interaction with nuclear DNA and parallel interactions in the cytoplasm [65-67], and so, in both cases, Raman micro-spectroscopy has shed further light on the current understanding of the mode of action of the clinically prescribed chemotherapeutic agents.

A.

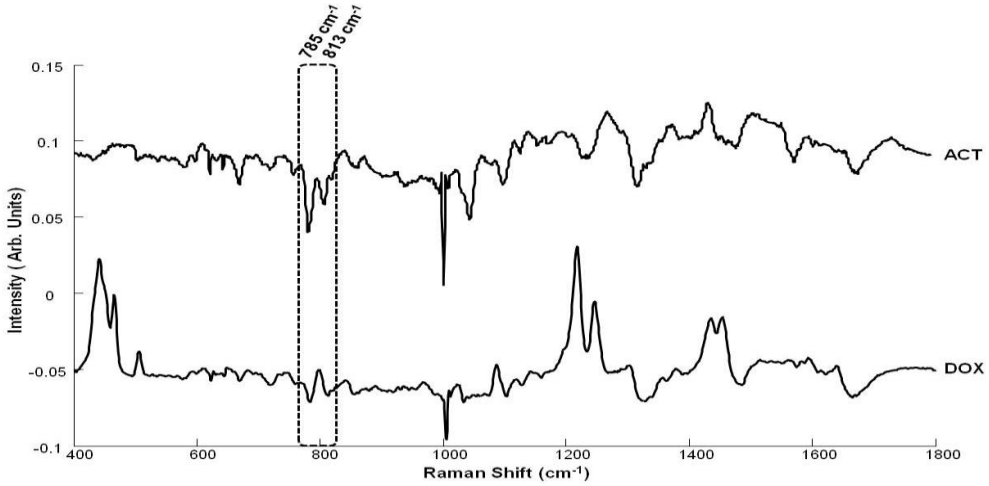

B.

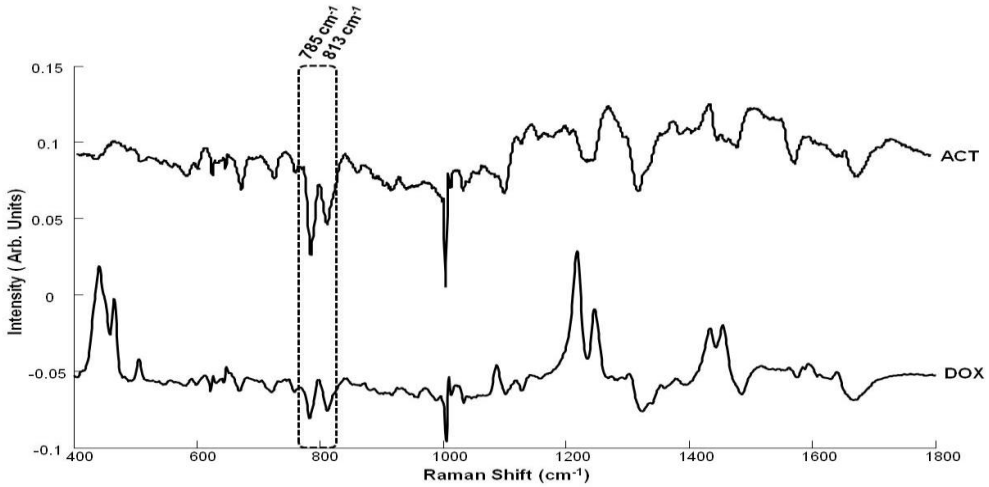

Figure 4: Loading 1 of PC1 of control versus exposed cells of Nucleolus **A.** A549 control versus 6hrs DOX exposure compared to that of control versus 48hrs exposure ACT **B.** Calu-1 control versus 2hrs DOX exposure compared to that of control versus 48hrs exposure ACT

Nawaz *et al.* [18, 68] explored the effects of Cisplatin (Cisp), which primarily interacts with DNA via inter-strand and intra-strand cross-links with purine bases, mostly by forming a 1,2-intrastrand cross-link between the N7 atoms of two adjacent guanine bases, on the Raman spectra of the nuclear region of A549 human lung adenocarcinoma cells after 96 hours exposure. The difference spectrum of cells exposed to the Cisp IC_{50} concentration and unexposed control cells reveals specific bands at, for example, 669 (thymine and guanine), 833 (DNA B form) and 1095 cm^{-1} (DNA PO_2- symmetric stretching), associated with intra-strand cross linkages between guanine/guanine and guanine/thymine, inducing conformational changes, consistent with the accepted mode of action of Cisp, as demonstrated also by Huang *et al.* [69], who monitored cellular apoptosis of nasopharyngeal carcinoma cells C666 after Cisp treatment. Using the drug dose and MTT cytotoxicity assay as independent regression targets in PLSR, Nawaz *et al.* [18, 68] showed that it was possible to distinguish cellular responses in the Raman spectrum as a result of Cisp interactions within the cell nucleus by chemical binding, and the subsequent cellular physiological response of the cell. Keating *et al.* [70] confirmed these results with simulated data, further emphasising the power of this technique, with application to High content analysis for *in vitro* drug testing.

It should be noted that, PLSR over the high concentration range , up to 50μM, (Figure 5A) results in a spectral profile which is similar to those of DOX and ACT (Figure 4) exhibiting strong features at 785 cm^{-1} (DNA backbone O–P–O) and 813 cm^{-1} (RNA O–P–O phosphodiester band stretching), while regression over the lower concentration up to the IC_{50} of 1.2 ± 0.2 μM showed a decrease in features at 728, 830 and 1425 cm^{-1}, related to DNA B form and an increase in features at 668 and 675 cm^{-1}, related to DNA A form, indicative of conformational changes due to partial transition of the DNA B-form to DNA A-form due to Cisp binding [18, 71, 72].

In acellular circular dichroism studies of drug DNA interactions, the spectral changes observed for the ACT-DNA complexes due to a B to A-type DNA transition upon interaction, are distinct from those of Cisp-DNA complexes, which reflect distortions in DNA of a nondenaturational nature [73]. Therefore, it is not expected that Cisp will induce similar conformational changes to DOX or ACT.

A.

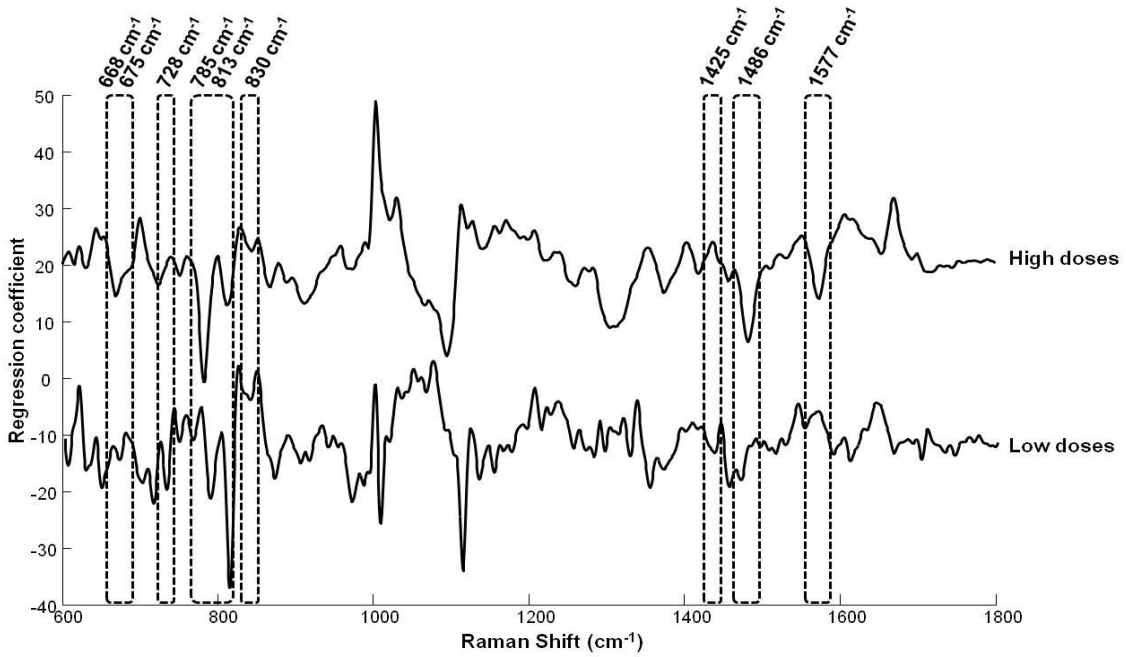

B.

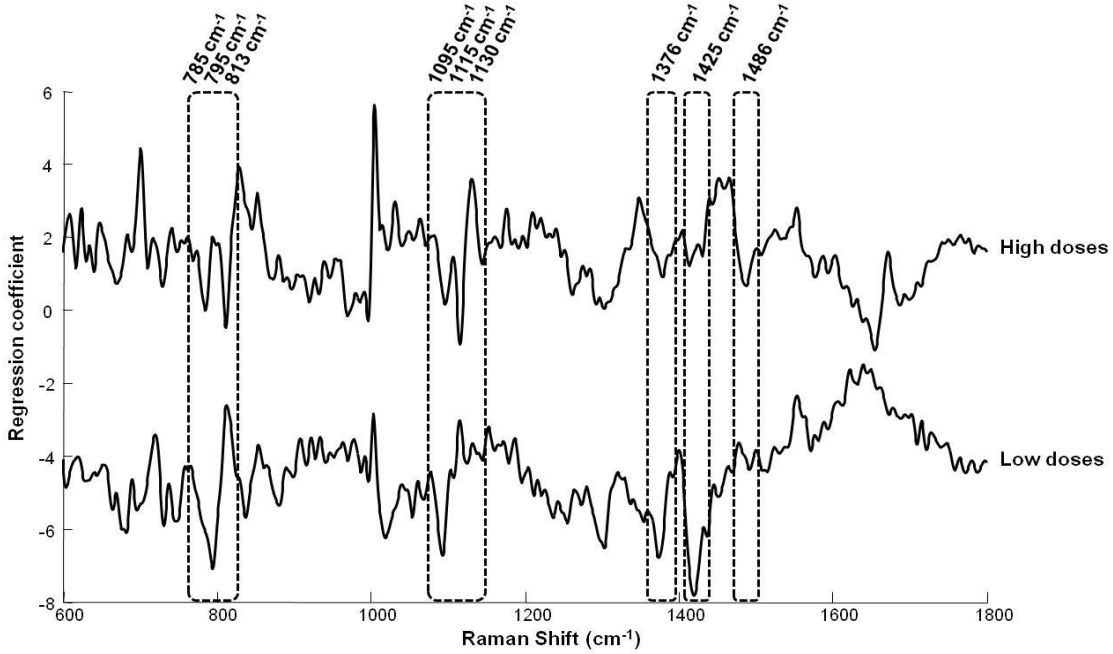

Figure 5: Regression coefficients obtained by PLSR analysis for A549 cell line as a function of drug dose at low and high doses for chemotherapeutic drugs **A.** Cisp and **B.** Vinc

In a similar, more recent, study of the effects of Vinc, Raman spectroscopy demonstrated that, as well as the accepted mechanism of action of microtubule binding, intercalation with nuclear DNA occurs at high doses [50]. Using Flow Cytometry to measure the anti-apoptotic bcl-2 protein expression reveals that it depends on the Vinc concentration; at low concentration, the

bcl-2 protein expression increases, inhibiting cell death by apoptosis and drops at higher concentrations due to higher levels of DNA damage. This is confirmed by a PLSR regression of the spectral responses of the nucleus versus Vinc dose at low and high doses, as shown in Figure 5B. At low doses (<IC_{50}), a single negative feature is observed at 795 cm^{-1}, whereas regression over the doses above the IC_{50} results in the double feature at 785 cm^{-1} and 810 cm^{-1}, characteristic of DNA intercalation and resultant conformational changes.

The studies of Cisp and Vinc demonstrate that a drug can have different modes of action, dependent on dose, [18, 50, 74, 75], and, indeed this is also demonstrated by the time evolution of the cellular DOX accumulation. Therefore, the characteristic spectroscopic signatures will vary as a function of dose, and exposure time, as also demonstrated by Moritz *et al.* [33], Schie *et al.* [34] and G*uo et al.* [35] for DOX exposure, although with different cell lines, doses and exposure times. Employing a clinically relevant exposure dose, and monitoring the evolution of the response, however, perhaps yields the best quality information, in terms of independently monitoring the drug accumulation, chemical binding and cellular responses.

Using Raman micro-spectroscopy and multivariate data analysis, in a similar fashion as Derenne *et al.*, drugs from the same chemotherapeutic group can be seen to exhibit similar chemical binding signatures which can be considered as a fingerprint of their mechanism of action, as shown by Farhane *et al.* [52] for the two anthracyclines DOX and ACT. Similar spectral signatures of the interaction with nucleic acids are observed in both the nucleolus and nucleus (Figure 4), consisting of a simultaneous decrease in the Raman features at 785 and 813 cm^{-1}, corresponding respectively to DNA backbone O–P–O and RNA O–P–O phosphodiester band stretching, despite the fact that they reveal different pharmacokinetics and different cellular resistance for different cell lines.

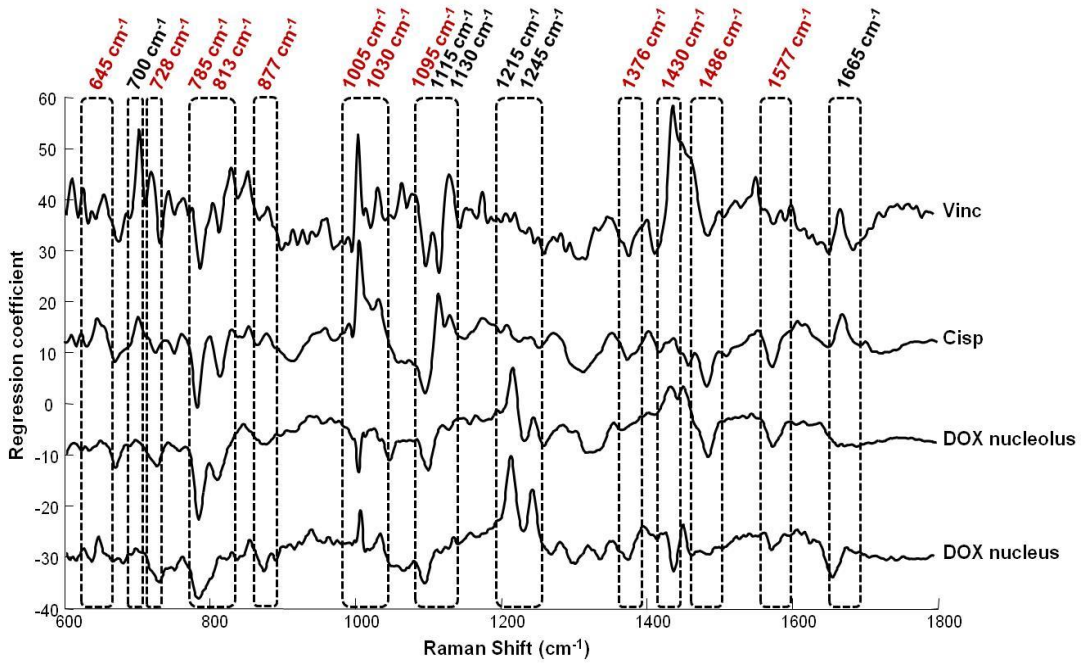

Figure 6: Regression coefficients obtained by PLSR analysis for A549 cell line as a function of drug dose for chemotherapeutic drugs DOX, Cisp and Vinc with common features highlighted on red

Similar decreases in both the Raman bands at 785 and 813 cm^{-1} were also observed for drugs from different chemotherapeutic groups (Figure 6): DOX, an anthracycline with high affinity for DNA, Cisp an alkylating agent which binds with DNA forming inter and intra strand crosslinks and Vinc, an alkaloid which bind to microtubules..

Despite the fact that those three chemotherapeutic drugs belong to different classes, they present a common mechanism of action by interaction with nucleic acids manifest in Raman analysis by the simultaneous decrease of features at 785 and 813 cm^{-1}. This can therefore be considered as a marker and a fingerprint of DNA intercalation and can be explored for new chemotherapeutic candidates. A similar decrease in features at 728 (adenine), 1095 (DNA PO_2- symmetric stretching), 1376 (thymine), 1486 and 1577 cm^{-1} (adenine and guanine) is also observed for the three drugs, indicating that they can interact with the four nucleic bases and bind externally with DNA.

The identification of such common spectroscopic signatures associated with a mode of action of these chemotherapeutic agents or cellular reactions can potentially be exploited for pre-clinical screening of the mode of action and potential resistance of new candidate chemotherapeutic agents.

Besides similar nucleic acids features, notable increases in protein features at 645 and 877 cm^{-1}, related to tyrosine, and 115-1130 cm^{-1}, related to C-N protein stretching, and lipids at 700 cm^{-1}, are also observed for the three drugs, which may be indicative of changes in protein structure and cellular resistance by synthesis of anti-apoptotic proteins and lipidic vesicules, as a way to remove DOX to the extracellular environment and thus could be considered as a marker of possible chemotherapeutic failure.

5. Raman micro-spectroscopy to distinguish cellular resistance

Farhane *et al.* [51], in a comparative study between the two lung cancer cell lines A549 and Calu-1 exposed to DOX at the dose corresponding to the IC_{50} of each, demonstrated that, despite the fact that there is a much faster uptake of DOX and cellular saturation in Calu-1 cells (Figure 3A and Figure 7B), they are more resistant than A549 cells and exhibit earlier evidence of a secondary mechanism of action of DOX, by ROS production [61]. In fact, Raman investigations show that the accumulation of DOX in the cytoplasmic area happens due to nuclear disruption, and as a consequence, the ROS production starts only after nuclear saturation, and that the two mechanisms of action, nucleic acid intercalation and ROS production, do not happen simultaneously. Further investigations demonstrate that, for both cells lines, there is a decrease in cellular features concomitant with DOX saturation, Calu-1 cells exhibiting higher DNA damage. However at later stages (Figure 3B and Figure 7B) in Calu-1 cells, there is a recovery of DNA and protein features, which suggests the intervention of DNA repair mechanisms and synthesis of anti-apoptotic proteins (confirmed by measurement of bcl-2, an anti-apoptotic protein and γH2AX, a marker of DNA damage and repair), both considered as mechanisms of cellular resistance. In fact, as seen in Figure 6 for A549 cells, there is an increase in γH2AX up to 24hrs corresponding to an increase in DNA damage and the increase in Bcl-2 protein is only up to 12hrs, with a continuous decrease in DNA, suggesting failure in anti-apoptosis and DNA recovery mechanisms. However, in Calu-1 cells, the bcl-2 expression continues to increase until the later stage of 48hrs, a decrease in γH2AX starting at 12hrs and a DNA recovery at late stages, consistent with a higher resistance than A549 cells (Figure 7).

A. **B.**

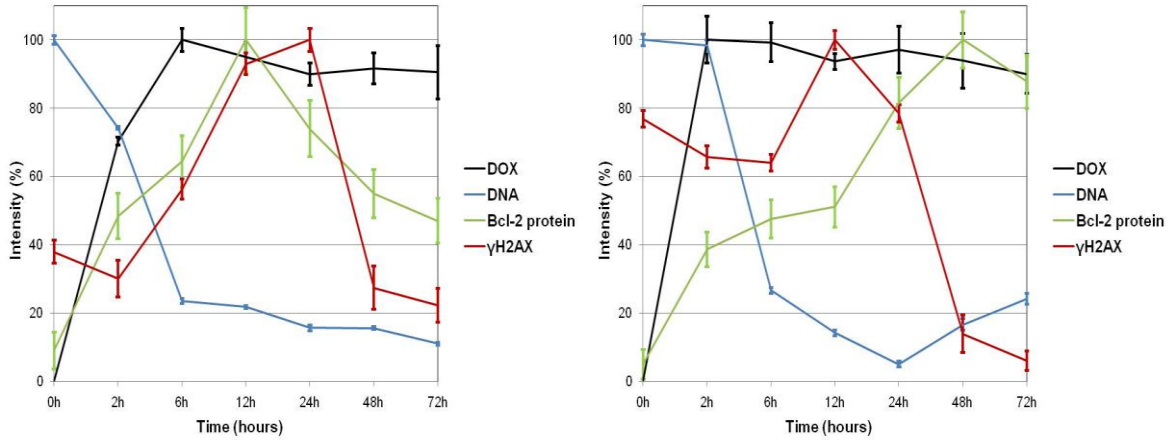

Figure 7: Evolution of DOX, represented by the Raman band at 465cm^{-1}, DNA, represented by the Raman band at 785 cm^{-1}, Bcl-2 protein and γH2AX expression, as measured by Flow Cytometry, as a function of time for the **A.** A549 and **B.** Calu-1 cell line. Intensities are expressed as percentage according to the maximum value for each parameter and for each cell line.

The cellular DNA repair capacity influences the efficacy of anticancer treatment and can be used as a biomarker of chemotherapeutic resistance. Moreover, resistance to apoptosis, programmed cell death, by either increase of anti-apoptotic protein, mainly bcl-2 proteins, or higher tolerance to DNA damage or DNA repair, as seen in Calu-1 cells, is associated with chemoresistance and as a consequence a poor clinical prognosis in cancer therapy and therefore can be used as a marker for individualised treatment.

A similar study by Farhane *et al.* [52], using ACT, also demonstrates the difference in chemosensitivity between A549 and Calu-1 cells. A higher viability and larger increase in protein features was observed in A549 cells, despite the fact that the two cell subtypes present similar ACT uptake rates.

The cell/drugs interaction induces different cellular reactions in the two cell lines, Calu-1 showing higher resistance for DOX and higher sensitivity for ACT. This difference in cellular reactions between cell lines and between the anthracyclines, as observed in protein features corresponding to synthesis of anti-apoptotic proteins and mobilisation of DNA repair proteins, may be due to differential drug retention rather than drug uptake, as ACT uptake is similar for the two cell lines and DOX uptake is faster in Calu-1 than A549 (which suggest higher sensitivity of Calu-1 to DOX than A549 and not the opposite).

The ability of Raman micro-spectroscopy to characterise and differentiate responses of resistant and sensitive cell types to drugs opens up potential clinical applications as a Companion Diagnostics tool, and ultimately personalised medicine approaches as a predictive tool for patient responses in individualised treatment.

6. Discussion:

Cytotoxicity assays are routinely employed to monitor the cellular viability and toxicity to external treatment individually or in a high content format. However, they give a limited insight into the mode of action and efficacy of drugs. In this context, Raman micro-spectroscopy can provide a label free alternative to high content analysis, potentially in real-time analysis with subcellular resolution and more profound understanding of mechanism of action of drugs and the subsequent cellular response pathways.

In the case of DOX, the IC_{50} concentration is high enough that it makes it possible to detect it inside cells and to monitor its uptake and accumulation at a subcellular level using Raman micro-spectroscopy. Investigations demonstrate that DOX accumulates and intercalates first in the nucleolus then in the nucleus, highlighting the important role of the nucleolus and the interaction with RNA in its mode of action, to our knowledge not previously demonstrated. It also shows that the secondary mechanisms of metabolisation in the cytoplasm causing oxidative stress only occur at later stages, after nuclear disruption, once the nuclear accumulation has saturated. Therefore, Raman micro-spectroscopy sheds light on the cellular interactions and medicinal chemistry, in situ, which were not previously known. Moreover, using multivariate data analysis, Raman spectroscopy is able to distinguish the signature of the binding interactions with the biochemical of the subcellular region from that of the subsequent cellular responses. Notably, different cell lines, exposed to the same chemotherapeutic drug DOX, show the same binding signatures, despite the fact that they exhibit different accumulation rates with different cellular resistances observed corresponding to synthesis of anti-apoptotic proteins, higher tolerance to DNA damage and implication of DNA repair mechanisms. In contrast, although structurally similar, ACT cannot be detected inside cell due to its low IC_{50}, of the order of nM compared to µM for DOX, which is indicative of its higher toxicity and efficacy. Nevertheless, it can be seen that ACT similarly interacts first in the nucleolus and then in the surrounding nucleus, albeit at a considerably slower rate, which is potentially due to the more bulky side chains of ACT slowing down its cellular transport and accumulation. Furthermore, similar Raman markers of cellular interactions are observed for

both anthracyclines, which indicates that Raman can potentially be used for the screening of the mode of action of drugs, to guide drug discovery and development research and in a pre-clinical screening context.

Moreover, Raman investigations demonstrate that different drugs can have different mechanisms of action, depending on applied dose, as observed for Cisp and Vinc, which at high doses are seen to intercalate with DNA, or as a function of time, as for example for DOX which induce different cellular responses (decrease and increase of cellular features specifically DNA, proteins and lipids) function of time, dose and cell lines. [1, 33-35, 51] Thus Raman can shed further light on understanding the mechanisms of action of known drugs with potential application in companion diagnostic.

The consistency of the spectroscopic signatures for drugs of similar modes of action, in different cell lines, suggests that this fingerprint can be considered a "spectralome" of the drug-cell interaction suggesting a new paradigm of representing spectroscopic responses. Notably, although the signature can contain features which can be associated with specific biomolecules, such as RNA, the full spectrum of that biomolecule is not manifest in the "spectralome", indicating that the spectral contributions can arise from conformational or other changes associated with the local environment of the biomolecule, and the "spectralome" also contains contributions of other molecules within that environment. In the absence of a labelling strategy, what you see is what you get, but the "spectralome", is a more holistic view of the biochemical changes associated with the drug-cell intereaction.

The ability of Raman micro-spectroscopy to characterise and differentiate responses of resistant and sensitive cell types to drugs opens up potential clinical applications as a Companion Diagnostics (CD) tool, and ultimately personalised medicine approaches [13, 42, 43]. The US Food and Drug Administration (FDA) defines CD as "a medical device, often an *in vitro* device (IVD), which provides information that is essential for the safe and effective use of a corresponding drug or biological product". Ultimately, the IVD should screen for patient specific suitability of therapeutic treatments, and both the FDA and the European Medicines Agency (EMA) now actively encourage the use of CD in the development and use of prescription drugs and even require CD marker testing prior to the prescription of certain drugs. Although more complex genomics based tests are emerging, most currently employed CD techniques are based on individual biomarkers in tissue or serum and, as is the case for fluorescent labels in microscopy, provide an extremely limited picture of the action of the drug and the cellular response. Emerging, more rapid spectroscopic screening technologies will afford more continuous and even real-time monitoring of such intracellular processes and

response pathways, which ultimately may be analysed using more sophisticated data mining techniques such as Multivariate Curve Resolution Alternating Least Squares. It can be projected, therefore, that Raman micro-spectroscopy can potentially contribute significantly to this field, by screening responses to identified therapeutics in patient derived cells, label-free, identifying signatures of cell resistance/sensitivity.

7. Conclusion:

The potential of Raman micro-spectroscopy not only to track *in vitro* the kinetics and accumulation of chemotherapeutic drugs at a subcellular level but also to identify their different mechanisms of action, for example via DNA intercalation and ROS production, according to different time points and doses and to identify factors contributing to chemotherapeutic resistance has been demonstrated.

In fact, Raman investigations show that drugs with similar mechanism of action, for example DNA intercalation, exhibit the same spectral signatures, which can be considered as a molecular fingerprint of their cellular interaction, opening the way to a new paradigm of in vitro analysis and characterisation, spectralomics. There is a dearth of techniques to visualise the action of drugs *in situ* in cells, and thus, Raman micro-spectroscopy can be used as an *in vitro* guide to medicinal chemistry strategies and a pre-clinical screening technique for drug mechanism of action and efficacy in order to aid preclinical drug development. Furthermore, the ability of Raman micro-spectroscopy to monitor subcellular processes associated with drug resistances suggests its potential as an in vitro companion diagnostics technique to screen for personalised therapies.

Acknowledgement:

This work was supported by Science Foundation Ireland Principle Investigator Award 11/PI/1108

References:

[1] Z. Farhane, F. Bonnier, A. Casey, and H.J. Byrne, Analyst **140,** 4212-4223 (2015).

[2] E. Efeoglu, A. Casey, and H.J. Byrne, Analyst **141,** 5417-5431 (2016).

[3] S.F. El-Mashtoly, H.K. Yosef, D. Petersen, L. Mavarani, A. Maghnouj, S. Hahn, G. Kotting, and K. Gerwert, Anal. Chem. **87,** 7297-7304 (2015).

[4] H.J. Byrne. *Biomedical Applications of Vibrational Spectroscopy Disease Diagnostics and Beyond*. in *Biomed Opt.* 2014. Miami, Florida: Optical Society of America.

[5] H.J. Byrne, K.M. Ostrowska, H. Nawaz, J. Dorney, A.D. Meade, F. Bonnier, and F.M. Lyng, *Vibrational Spectroscopy: Disease Diagnostics and Beyond*, in *Optical Spectroscopy and Computational Methods in Biology and Medicine*, M. Baranska, Editor. 2013, Springer Netherlands: Dordrecht. p. 355-399.

[6] F. Bonnier, A. Mehmood, P. Knief, A.D. Meade, W. Hornebeck, H. Lambkin, K. Flynn, V. McDonagh, C. Healy, T.C. Lee, F.M. Lyng, and H.J. Byrne, J. Raman Spectrosc. **42,** 888-896 (2010).

[7] F. Bonnier, S.M. Ali, P. Knief, H. Lambkin, K. Flynn, V. McDonagh, C. Healy, T.C. Lee, F.M. Lyng, and H.J. Byrne, Vibrational Spectroscopy **61,** 124-132 (2012).

[8] T. Huser and J. Chan, Adv Drug Deliv Rev. **89,** 57-70 (2015).

[9] Z. Farhane, F. Bonnier, A. Casey, A. Maguire, L. O'Neill, and H.J. Byrne, Analyst **140,** 5908-5919 (2015).

[10] F. Bonnier, F. Petitjean, M.J. Baker, and H.J. Byrne, J.Biophotonics **7,** 167-179 (2014).

[11] A.A. Bunaciu, A. Fleschin, V.D. Hoang, and H.Y. Aboul-Enein, Crit Rev Anal Chem **47,** 67-75 (2017).

[12] S.H. Cho, J. Jeon, and S.I. Kim, J Breast Cancer **15,** 265-272 (2012).

[13] C.L. Overby and P. Tarczy-Hornoch, Per Med. **10,** 453-462 (2013).

[14] D.R. Whelan, K.R. Bambery, L. Puskar, D. McNaughton, and B.R. Wood, Analyst **138,** 3891-3899 (2013).

[15] F. Bonnier, P. Knief, B. Lim B, A.D. Meade, J. Dorney, K. Bhattacharya, F. Lyng, and H.J. Byrne, Analyst **135,** 3169-3177 (2010).

[16] A.D. Meade, C. Clarke, F. Draux, G.D. Sockalingum, M. Manfait, F. Lyng, and H.J. Byrne, Anal Bioanal Chem **5,** 1781-1791 (2010).

[17] C. Hughes, G. Clemens, and M.J. Baker, Trends Biotechnol **33,** 429-430 (2015).

[18] H. Nawaz, H., F. Bonnier, P. Knief, O. Howe, F. Lyng, A.D. Meade, and H.J. Byrne, Analyst **135,** 3070-3076 (2010).

[19] A. Derenne, R. Gasper, and E. Goormaghtigh, Analyst **136,** 1134-1141 (2011).

[20] A. Derenne, V. Van Hemelryck, D. Lamoral-Theys, R. Kiss, and E. Goormaghtigh, Biochim Biophys Acta **1832,** 46-56 (2013).

[21] R. Gasper, T. Mijatovic, A. Bénard, A. Derenne, R. Kiss, and E. Goormaghtigh, Biochim Biophys Acta **1802,** 1087-1094 (2010).

[22] F. Nie, X.L. Yu, X.G. Wang, Y.F. Tang, L.L. Wang, and L. Ma, Int J Oncol **37,** 1261-1269 (2010).

[23] A. Mignolet, A. Derenne, M. Smolina, B.R. Wood, and E. Goormaghtigh, Biochim Biophys Acta **1864,** 85-101 (2016).

[24] L.E. Jamieson and H.J. Byrne, Vib. Spectrosc. **DOI: 10.1016/j.vibspec.2016.09.003,** (2016).

[25] A. Derenne, M. Verdonck, and E. Goormaghtigh, Analyst **137,** 3255-3264 (2012).

[26] S.M. Ali, F. Bonnier, H. Lambkin, K. Flynn, V. McDonagh, C. Healy, T.C. Lee, F.M. Lyng, and H.J. Byrne, Anal. Methods **5,** 2281-2291 (2013).

[27] S.F. El-Mashtoly, D. Petersen, H.K. Yosef, A. Mosig, A. Reinacher-Schick, C. Kotting, and K. Gerwert, Analyst **139,** 1155-1161 (2014).

[28] K. le Roux, L. C. Prinsloo, and D. Meyer, Appl. Phys. Lett. **105,** 123702 (2014).

[29] H. Salehi, L. Derely, A.G. Vegh, J.C. Durand, C. Gergely, C. Larroque, M.A. Fauroux, and F.J.G. Cuisinier, Appl. Phys. Lett. **102,** 113701 (2013).

[30] H. Salehi, E. Middendorp, I. Panayotov, P.Y. Collart Dutilleul, A.G. Vegh, S. Ramakrishnan, C. Gergely, and F. Cuisinier, J Biomed Opt **18,** 56010 (2013).

[31] A.V. Feofanov, A.I. Grichine, L.A. Shitova, T.A. Karmakova, R.I. Yakubovskaya, M. Egret-Charlier, and P. Vigny, Biophys. J. **78,** 499-512 (2000).

[32] F. Draux, C. Gobinet, J. Sule-Suso, M. Manfait, P. Jeannesson, and G.D. Sockalingum, Analyst **136,** 2718-2725 (2011).

[33] T.J. Moritz, D.S. Taylor, D.M. Krol, J. Fritch, and J.W. Chan, Biomed. Opt. Express **1,** 1138-1147 (2010).

[34] I.W. Schie, L. Alber, A.L. Gryshuk, and J.W. Chan, Analyst **139,** 2726-2733 (2014).

[35] J. Guo, W. Cai, B. Du, M. Qian, and Z. Sun, Biophys Chem **140,** 57-61 (2009).

[36] K. Hartmann, M. Becker-Putsche, T. Bocklitz, K. Pachmann, A. Niendorf, P. Rösch, and J. Popp, Anal. Bioanal. Chem. **403,** 745-753 (2012).

[37] D. Lin, J. Lin, Y. Wu, S. Feng, Y. Li, Y. Yu, G. Xi, H. Zeng, and R. Chen, Spectroscopy **25,** (2011).

[38] A. Zoladek, F.C. Pascut, P. Patel, and I. Notingher, J. Raman Spectrosc. **42,** 251-258 (2011).

[39] H.K. Yosef, L. Mavarani, A. Maghnouj, S. Hahn, S.F. El-Mashtoly, and K. Gerwert, Anal Bioanal Chem **407,** 8321-8331 (2015).

[40] A.V. Rutter, M.R. Siddique, J. Filik, C. Sandt, P. Dumas, G. Cinque, G.D. Sockalingum, Y. Yang, and J. Sulé-Suso, Cytometry Part A **85,** 688-697 (2014).

[41] M.R. Siddique, A.V. Rutter, K. Wehbe, G. Cinque, G. Bellisola, and J. Sule-Suso, Analyst **142,** 1299-1307 (2017).

[42] A. Agarwal, D. Ressler, and G. Snyder, Pharmgenomics Pers Med **8,** 99-110 (2015).

[43] S. Naylor and T. Cole, Drug Discovery World **Spring 2010,** 67-69 (2010).

[44] M.J. Baker, R. Goodacre, C. Sammon, M.P. Marques, P. Gardner, W. Tipping, J. Sule-Suso, B. Wood, H.J. Byrne, M. Hermes, P. Matousek, C.J. Campbell, S. El-Mashtoly, J. Frost, C. Phillips, M. M. Diem, A. Kohler, K. Lau, S. Kazarian, W. Petrich, G. Lloyd, I. Delfino, G. Cinque, M.Isabelle, N. Stone, C. Kendall, L. Jamieson, D. Perez-Guaita, L. Clark, K. Gerwert, I. Notingher, L. Quaroni, R. Bhargava, A. Meade, and F. Lyng, Faraday Discussions **187,** 299-327 (2016).

[45] M.A. Maher, P. Naha, S.P. Mukherjee, and H.J. Byrne, Toxicol in Vitro **28,** 1449-1460 (2014).

[46] G. Repetto, A. del Peso, and J.L. Zurita, Nat Protoc **7,** 1125-1131 (2008).

[47] R. Hamid, Y. Rotshteyn, L. Rabadi, R. Parikh, and P. Bullock, Toxicol In Vitro **18,** (2004).

[48] S. Al-Nasiry, N. Geusens, M. Hanssens, C. Luyten, and R. Pijnenborg, Human Reproduction **22,** 1304-1309 (2007).

[49] R.D. Fields and M.D. Lancaster, Am Biotechnol Lab **11,** 48-50 (1993).

[50] H. Nawaz, H., A. Garcia, A.D. Meade, F. Lyng, and H.J. Byrne, Analyst **138,** 6177-6184 (2013).

[51] Z. Farhane, F. Bonnier, O. Howe, A. Casey, and H.J. Byrne, J Biophotonics **doi: 10.1002/jbio.201700060,** n/a-n/a (2017).

[52] Z. Farhane, F. Bonnier, and H.J. Byrne, J Biophotonics **doi: 10.1002/jbio.201700112,** n/a-n/a (2017).

[53] D. Ragnvaldsson, R. Berglind, M. Tysklind, and P. Leffler, Ambio. **36,** 494-501 (2007).

[54] C. Wittwehr, H. Aladjov, G. Ankley, H.J. Byrne, J. de Knecht, E. Heinzle, G. Klambauer, B. Landesmann, M. Luijten, C. MacKay, G. Maxwell, M.E. Meek, A. Paini, E. Perkins,

T. Sobanski, D. Villeneuve, K.M. Waters, and M. Whelan, Toxicological Sciences **155,** 326-336 (2017).

[55] H.J. Byrne, P. Knief, M.E. Keating, and F. Bonnier, Chem Soc Rev **45,** 1865-1878 (2016).

[56] L.T. Kerr, H.J. Byrne, and B.M. Hennelly, Anal Methods **7,** 5041-5052 (2015).

[57] O. Ibrahim, A. Maguire, A.D. Meade, S. Flint, M. Toner, H.J. Byrne, and F.M. Lyng, Anal Methods **9,** 4709-4717 (2017).

[58] L.T. Kerr and B.M. Hennelly, Chemometr. Intell. Lab **158,** 61-68 (2016).

[59] I.W. Schie and J.W. Chan, J. Raman Spectrosc. **47,** 384-390 (2016).

[60] F. Bonnier and H.J. Byrne, Analyst **137,** 322-332 (2012).

[61] Z. Farhane, F. Bonnier, M.A. Maher, J. Bryant, A. Casey, and H.J. Byrne, J Biophotonics **10,** 151-165 (2017).

[62] T.W. Lee, *Independent Component Analysis*, in *Independent Component Analysis: Theory and Applications*. 1998, Springer US: Boston, MA. p. 27-66.

[63] Z. Farhane, F. Bonnier, and H.J. Byrne, Anal Bioanal Chem **409,** 1333-1346 (2017).

[64] K. Dana, C. Shende, H. Huang, and S. Farquharson, Journal of analytical & bioanalytical techniques **6,** 1-5 (2015).

[65] A. Rabbani, R.M. Finn, and J. Ausió, BioEssays **27,** 50-56 (2005).

[66] G. Minotti, P. Menna, E. Salvatorelli, G. Cairo, and L. Gianni, Pharmacol. Rev **56,** 185 (2004).

[67] F. Yaqub, The Lancet Oncology **14,** e296 (2013).

[68] H. Nawaz, F. Bonnier, A.D. Meade, F.M. Lyng, and H.J. Byrne, Analyst. **136,** 2450-2463 (2011).

[69] H. Huang, H. Shi, S. Feng, W. Chen, Y. Yu, D. Lin, and R. Chen, Anal. Methods **5,** 260-266 (2013).

[70] M.E. Keating, H. Nawaz, F. Bonnier, and H.J. Byrne, Analyst **140,** 2482-2492 (2015).

[71] D. Ghosh, S.K. Dey, and C. Saha, PLoS ONE **9,** e84880 (2014).

[72] V. Vaverkova, O. Vrana, V. Adam, T. Pekarek, J. Jampilek, and P. Babula, BioMed Res. Int **2014,** 12 (2014).

[73] Y.M. Chang, C.K. Chen, and M.H. Hou, Int J Mol Sci. **13,** 3394-3413 (2012).

[74] A. Mohammadgholi, A. Rabbani-Chadegani, and S. Fallah, DNA and Cell Biology **32,** 228-235 (2012).

[75] G. Tyagi, D.K. Jangir, P. Singh, and R. Mehrotra, DNA Cell Biol **29,** 693-699 (2010).